Journal of Thermal Analysis and Calorimetry (2021) 145:649–657
https://doi.org/10.1007/s10973-020-10004-6

Performance assessment of the photon enhanced thermionic emitter and heat engine system

Emin Açıkkalp[1] · **Süheyla Yerel Kandemir**[2]

Received: 27 April 2020 / Accepted: 27 June 2020 / Published online: 12 July 2020

Abstract
The aim of this research is to show the potential application of a photon enhanced thermionic emitter (PETE)–irreversible heat engine (HE) hybrid system. Solar energy has the greatest potential for clean energy, and thermionic emission is the alternative way to convert heat and light into electricity. PETE is an efficient solar to electricity converter comparing to other solar converters, which its efficiency can reach above 50%. Briefly, PETE–heat engine system is analyzed, where the PETE is the main cycle and HE is the bottom cycle. Receiving temperature to PETE above 1000 K and this heat can be utilized by a bottom cycle, heat rejected by the PETE is used by the heat engine, and additional power output is obtained. In addition to basic performance evaluation consisting of power output and electricity efficiency, some exergetic parameters are considered. These exergetic parameters can be listed as: exergy efficiency, depletion ratio, waste exergy ratio, exergetic sustainability index, exergetic ecological index, and modified exergetic ecological index. According to the results, power output, energy efficiency, exergy efficiency, sustainability index, ecological exergetic index, and modified ecological index are 63.698 W cm^{-2}, 0.637, 0.721, 2.603, 0.652, and 0.477, for the optimum cathode temperature and for the optimum anode work function are 67.295 W cm^{-2}, 0.673, 0.764, 3.312, 0.735, and 0.616 are possible to be achieved.

Keywords Photon enhanced thermionic emission · Irreversible heat engine · Exergy · Performance · Exergetic indicators

Introduction

For last decades, there has been a great effort to harness solar power not only generating heat but also electricity. Sun is the source of life and energy in the world, and it is a certain solution to the increasing energy needs and environmental issues. There are many ways to generate electricity from the sun like concentrated or non-concentrated PV panels, solar dish Stirling engine, concentrated solar thermal power, thermoelectric generators, etc. Solar thermionic devices are relatively new and efficient technology called as photon enhanced thermionic emission (PETE) device. It is based on the thermionic cycle device which converts heat to electricity. Their typical cathode temperature is higher than 1000 °C.

✉ Emin Açıkkalp
eacikkalp@gmail.com; emin.acikkalp@bilecik.edu.tr

[1] Department of Mechanical Engineering, Engineering Faculty, Bilecik S.E. University, Bilecik, Turkey

[2] Department of Industrial Engineering, Engineering Faculty, Bilecik S.E. University, Bilecik, Turkey

PETE was firstly proposed by the Schwede et al. [1], investigated the performance of the PETE and an ideal heat engine combination. The results pointed that more than 50% energy efficiency can be achieved theoretically for the system. Segev et al. [2] searched the energy efficiency of the photon enhanced thermionic emission solar converters. They showed that the efficiency of the PETE had the possibility to reach above 40%. Reck and Hensen [3] presented a thermodynamic model for the PETE. Su et al. [4] performed a parametric investigation of the PETE to determine optimum operating conditions. Su et al. [5] analyzed the effect of the space charge on efficiency, and they made parametric design. Si, GaAs, and InP were compared to each other as cathode materials in Ref. [6], and it is found that InP is promising material according to efficiency. Wang et al. [7] analyzed the effect of the nanoscale vacuum gap on the PETE. They concluded that it has a strong effect on the energy efficiency of the PETE. Segev et al. [8] compared the theoretical efficiencies of the PETE, PV, and thermal-electric conversion. The results showed that the theoretical efficiency of the PETE can reach 56% and 70.4% with a bottom cycle. Xiao et al. [9] made thermodynamic analysis of PETE and the

PETE–Carnot heat engine combination. They considered exergy efficiency, exergy ratio, entropy change, and power output. Açıkkalp et al. [10] researched a thermophotovoltaic-driven thermionic refrigerator. The system is analyzed for power output, COP, exergy destruction, and exergy efficiency. According to the results, it is achievable that the cooling load is 648 W m^{-2}, exergy efficiency is 0.071, and COP is 3.5.

Exergy analysis is assumed as very powerful tool in designing, modeling, and evaluating of an energy converter. It takes an opportunity to scientists or engineers to find and improve inefficiencies and losses in a system. It can be applied in a wide range to heat exchanger to power plants. Some examples of application of the exergy analysis can be found in refs. [11–26]. Another useful method is the ecological function presented by Angulo-Brown [27] and improved by Yan [28]. This method aims to maximize the difference of power output and exergy destruction rate.

In this research, a PETE and an irreversible HE hybrid system is considered. In the literature, the most study is focused on material, single performance of the PETE, and there is a few study hybrid usages of the PETE, which consider the reversible or ideal cycles. In this paper, irreversible PETE–HE hybrid system was analyzed in detail. In addition to the basic performance analysis, which are efficiency and power output, the system is analyzed by using some exergetic indicators including exergy efficiency, depletion ratio, waste exergy ratio, exergetic sustainability index, exergetic ecological index, and modified exergetic ecological index. Exergetic ecological index is relatively new, and the modified exergetic ecological index is presented firstly in this study. According to the author's knowledge, such a PETE–irreversible heat engine system analyzed in detail first time in the literature.

System description and evaluation criteria

A photon enhanced thermionic converter has basically the same principle with a simple thermionic converter. This principle can be explained as follows; it involves two electrodes, which are called cathode and anode, and metallic materials, separating with vacuum space and connected with an external load. When the cathode is heated and electrons have enough energy to overcome the potential barrier, it emits electrons into the vacuum and these are collected by the anode, and, in the final step, they are conveyed to the external load. In the photon enhanced thermionic emission converter, the metallic cathode material is changed with the *p*-type semiconductor band gap that is matched to the solar spectrum and with low electron affinity at its electron emission surface. When illuminated with concentrated solar energy, photo-generation increases the conduction band electron population above the equilibrium level, and the emission energy barrier is reduced. As a result, more electrons are emitted from the cathode at lower cathode temperatures compared to conventional thermionic emitters [8]. After the generating electricity, waste heat can be utilized by a heat engine. In this article, a PETE–HE system shown in Fig. 1 is investigated in terms of performance. Performance analysis is not only conducted for the power output and energy efficiency, which are subjected to the energy analysis but also some exergetic-based criteria are considered. Analysis of any energy conversion system would not complete without exergetic methods since exergy-based analyses provide knowledge about how efficient energy sources are used. This is important, because, using energy resources more efficient means that same amount of power comparing to heat engines operating under the same conditions is generated utilizing less energy input or fuel. It is obvious that it has more advantageous in terms of environmentally and economically.

Exergy efficiency, depletion ratio, waste exergy rate, exergetic sustainability index, exergetic ecological index, and modified exergetic ecological index are considered for

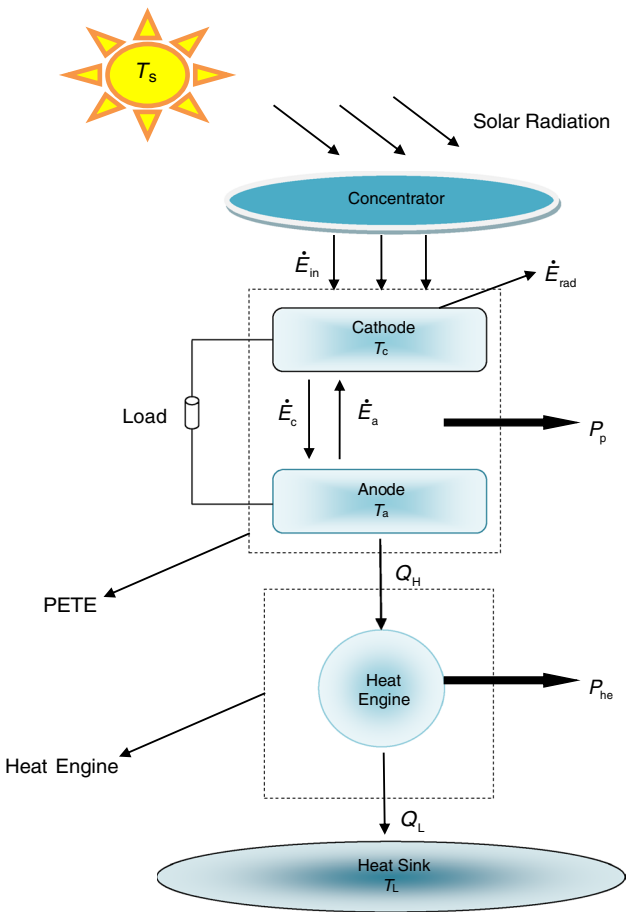

Fig. 1 Schematic of the PETE–HE hybrid system

exergetic assessment. Exergy efficiency is the measure of how an energy conversion device is close to an ideal cycle. Ideal cycle can be described as a cycle having the maximum efficiency, and there is no lost exergy (such as power output). The greater exergy efficiency means the greater energy efficiency too. The depletion ratio is the ratio of the exergy destruction raterate to the exergy input (or fuel exergy). This is an indicator to show how much input exergy is depleted or destructed, which cannot be recovered. Similarly, the waste exergy ratio is the ratio of the sum of the exergy destruction rate and exergy loss to exergy input. Exergy loss can be defined as a rejected exergy from the system, and it cannot be utilized by the system itself, but it can be utilized by another system. Exergetic ecological index was proposed Açıkkalp and Ahmadi [29] adopted from the ecological function [27, 28]. Exergetic ecological index is described as difference of the exergy efficiency and depletion ratio. This index provides not only a comparison of the useful and wasted power but also comparison with the consumption of the exergy source. In addition, exergetic ecological index includes all exergetic parameters and enables us to evaluate a considered system using all exergetic parameters [16]. This index could have negative values, and these points have resulted from the fact that the exergy destruction rate is bigger than the power output and these points are needed to avoid. In this paper, modified exergetic ecological index is proposed first time. The difference of this index is that it contains exergy destruction rate and exergy lost together. In this way, it is aimed to consider all losses in the system.

Analysis

The first step is to analyze PETE. According to conversion of the energy, Eq. (1) can be written for the PETE:

$$\dot{E}_{in} - P_p - \dot{E}_{rad} - \dot{Q}_H = 0 \tag{1}$$

here $\dot{E}_{in}, P_p, \dot{E}_{rad}, \dot{Q}_H$ are the input power or solar power, power output from the PETE, radiation energy flux, and heat rejected from the PETE, respectively. Input power (W) can be expressed as follows:

$$\dot{E}_{in} = CP_s \tag{2}$$

where C is the concentration ratio and P_s are the AM1.5 direct circumsolar spectrum. Power output from the PETE (W) is described in Eq. (3):

$$P_p = \left(j_c - j_a\right)V \tag{3}$$

in this equation, j_c (A/cm^2) is the cathode current density, j_a (A/cm^2) is the cathode current density, and V is the voltage radiation energy flux (W) is:

$$\dot{E}_{rad} = \int_{E_g}^{\infty} \frac{(h\nu)^3 \mathrm{d}(h\nu)}{\left(e^{h\nu/kT_c} - 1\right)} \tag{4}$$

where h (Js) is the Planck's constant, $h\nu$ (J) is the photon energy, k (J/K) is the Boltzmann constant, and T_c (K) is the cathode temperature. Heat rejected from the PETE (W):

$$\dot{Q}_H = j_c\left(\Phi_a + 2kT_c\right) - j_a\left(\Phi_a + 2kT_a\right) \tag{5}$$

where Φ_a(eV) is the work function of anode and T_a (K) is the anode temperature. Cathode and anode current densities are:

$$j_c = en\sqrt{\frac{kT_c}{2\pi m_e}}\mathrm{e}^{-\chi/kT_c} \tag{6}$$

$$j_a = A_o T_a^2 \mathrm{e}^{-\Phi_a/kT_a} \tag{7}$$

e is the electron charge (Coulomb), n is overall conduction band electron density, m_e (kg) is the mass of electron, and χ is the electron affinity. Photon enhanced conduction band electron density is defined as:

$$\mathrm{d}n = n - n_{eq} = \frac{\left[K_p + K_{bb}\left(n_{eq} + p_{eq}\right)\right] + \sqrt{\left[K_p + K_{bb}\left(n_{eq} + p_{\partial}\right)\right]^2 - 4K_{bb}\left[\Gamma - K_p n_{eq}\right]}}{2K_{bb}} \tag{8}$$

where n_{eq} equilibrium electron density, p_{eq} equilibrium hole density, K_p is the coefficient at which electrons emit per volume, K_{bb} is the coefficient at which electrons recombine per volume, and Γ is the rate of photoexcitation. n_{eq} and p_{eq} are calculated by using Eqs. (9)–(15):

$$n_{eq} = n_c \mathrm{e}^{-(E_g - E_f)/kT_c} \tag{9}$$

$$p_{eq} = n_v \mathrm{e}^{(-E_f)/kT_c} \tag{10}$$

$$n_c = 2\left(\frac{2\pi m_n^* kT_c}{h^2}\right)^{3/2} \tag{11}$$

$$n_v = 2\left(\frac{2\pi m_p^* kT_c}{h^2}\right)^{3/2} \tag{12}$$

$$n_i = \sqrt{n_c n_v}\, e^{\left(-\frac{E_g q_o}{kT_c}\right)} \tag{13}$$

$$E_g = 1.17 - \frac{4.73\times 10^{-4} T_c^2}{T_c + 636} \tag{14}$$

$$E_f = \frac{E_g}{2} + \frac{kT_c}{2}\ln\left(\frac{10^{19}}{n_i}\right) \tag{15}$$

here E_g (eV) is the band gap energy, E_f (eV) is the Fermi energy, n_c and n_v are the effective densities of states in the conduction band and valence respectively, and n_i is the intrinsic carrier concentration. Work function of the cathode (eV) is:

$$\Phi_c = \chi + E_g - E_f \tag{16}$$

overall conduction band electron and hole densities are written in Eq. (17):

$$n = dn + n_{eq}, \quad p = dn + p_{eq} \tag{17}$$

Secondly, heat engine part is analyzed. Heat input and rejected heat (W) can be defined as follows, respectively [30]:

$$\dot{Q}_H = \frac{z\left(T_a x - T_L\right)y}{(1+y)(Ix+y)} \tag{18}$$

$$\dot{Q}_L = Ix\dot{Q}_H \tag{19}$$

y is the ratio of heat conductance, z is the sum of heat conductance (J/K), x is the ratio of the temperature of the working fluids, and I is the parameter of internal irreversibility. Power output of the heat engine (W) can be described as:

$$P_{he} = \dot{Q}_H - \dot{Q}_L \tag{20}$$

Energy efficiencies are:

$$\eta_p = \frac{P_p}{\dot{E}_{in}}, \quad \eta_{he} = \frac{P_{he}}{\dot{Q}_H} \tag{21}$$

Exergy input is equal to exergy of the Sun (eV), and it is [9]:

$$\dot{E}x_s = \left(CP_s\right)\left(1 - \frac{4T_o}{3T_s} + \frac{T_o^4}{3T_s^4}\right) \tag{22}$$

Exergy destruction rate (eV) is:

$$\dot{E}xd_p = T_o\frac{\dot{E}_{in}}{T_s}\left(1 - \eta_p - \frac{T_{H,f}}{T_s}\right), \quad \dot{E}xd_{he} = T_o\frac{\dot{Q}_H}{T_s}\left(1 - \eta_{he} - \frac{T_L}{T_a}\right) \tag{23}$$

Exergy efficiencies are:

$$\varphi_p = \frac{P_p}{\dot{E}x_s}, \quad \varphi_{he} = \frac{P_{he}}{\dot{Q}_H\left(1 - \frac{T_L}{T_a}\right)} \tag{24}$$

Ecological exergetic index, modified ecological exergetic index, depletion ratio, waste exergy ratio, and sustainability index are:

$$\lambda = \varphi - \omega, \quad \delta = \varphi - \varepsilon, \quad \omega = \frac{\dot{E}xd}{\dot{E}x_s},$$
$$\varepsilon = \frac{\dot{E}xd + \dot{E}x_{loss}}{\dot{E}x_s}, \quad \sigma = \frac{P}{\dot{E}xd + \dot{E}x_{loss}} \tag{25}$$

Finally, power output, energy efficiency, exergy efficiency , and exergy destruction raterates for the hybrid system:

$$P_h = P_p + P_{he}, \quad \eta_h = \frac{P_p + P_{he}}{\dot{E}_{in}},$$
$$\varphi_h = \frac{P_p + P_{he}}{\dot{E}x_s}, \quad \dot{E}xd_h = \dot{E}xd_p + \dot{E}xd_{he} \tag{26}$$

Results and discussion

This paper is about the investigation of performance, sustainability, and environment effect of the PETE–HE hybrid system, which exergetic, sustainable, and environmental effect parameters are researched for the H. These parameters

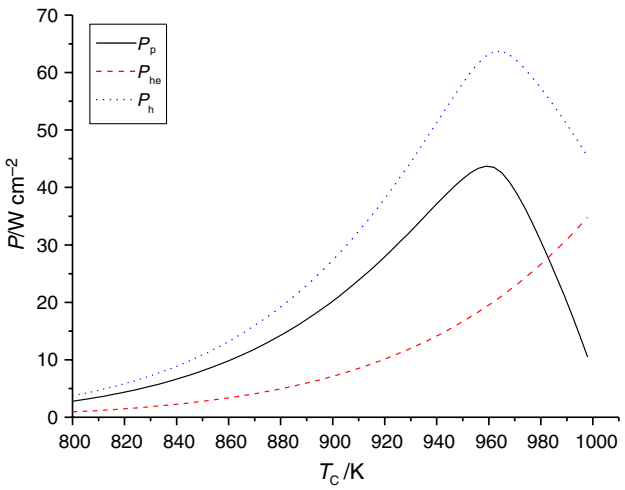

Fig. 2 Changes of the power densities with cathode temperature

are exergy efficiency, exergetic ecological index, modified exergetic ecological index, depletion ratio, waste exergy recovery ratio, and sustainability index. In the following, it can be found that parameters, which are chosen from the literature [1–9], $A_o = 120$ A cm^{-2} K^{-2}, $\Gamma = 0$, $T_o = 300$ K, $T_S = 5700$ K, $\Phi_A = 0.9$ eV, $T_C = 1000$ K, $L = 2 \times 10^{-7}$ cm, $\chi = 0.5$ eV, $y = 1$, $z = 300$ W cm^{-2} K, $I = 1.05$.

Figure 2 shows the influence of the cathode temperature on the power densities. It is a well-known truth that the energy gap of the cathode is dependent on the temperature strictly [see Eq. (14)] and the energy gap is one of the most important variables for the PETE. The range of the cathode temperature is chosen and researched between 800 and 1000 K. Voltage and current of the PETE are dramatically dependent on the cathode temperature. These parameters are inversely proportional to each other. Since there is an extremum point of the power density for the PETE [see Eq. (3)], as can be seen in Fig. 3, PETE and hybrid systems have the maximum points at cathode temperature which are equal to 959 K and 965 K, respectively. Corresponding power densities are 43.686 W cm^{-2} for the PETE and 63.698 W cm^{-2} for the hybrid system. The power density of the heat engine changes from 0.940 to 39.092 W cm^{-2} under considered temperatures. The trend of the energy efficiencies is depicted in Fig. 4. Like power densities, energy efficiencies of the PETE and hybrid system have the maximum points, which can be called as the optimum point. Maximum energy efficiencies of PETE and hybrid systems are obtained at 959 K and 965 K, which are equal to 0.437 and 0.637, respectively. When investigated energy efficiencies of the HE, one can see that it can be ignored and assumed as constant. The reason for this stability can explain that variation in the heat input and power output of the HE is the same. The energy efficiency of the HE is 0.416. Exergy

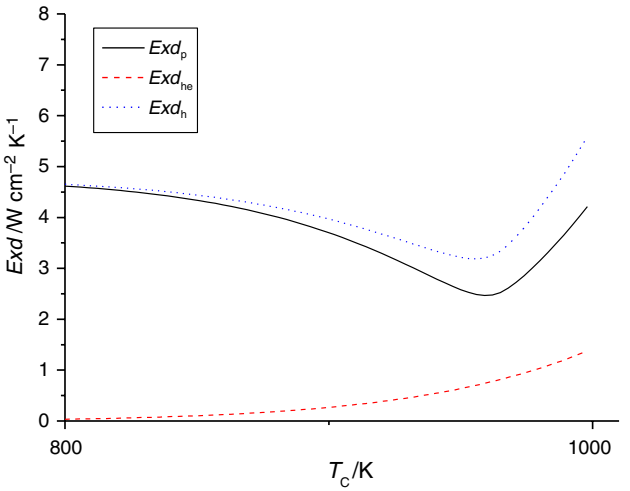

Fig. 4 Changes of exergy destruction raterate densities with cathode temperature

destruction rate densities are revealed in Fig. 5. PETE and hybrid systems have minimum points, it is an expected result. According to Eq. (23), it can be easily seen that higher efficiency causes the lower exergy destruction. Since these points may be called as optimum points for exergy destruction rate because inefficiencies of the considered system is decreased, in this way, power output and energy efficiency are increased. However, the exergy destruction rate density rate of the hybrid system is not minimum at the place where energy efficiency is the maximum. The minimum exergy destruction rate density for the PETE is 2.466 W cm^{-2} K^{-1} and 3.188 W cm^{-2} K^{-1} for the hybrid system. One can see that the exergy destruction rate density of the HE increases. The exergy destruction rate values of the HE are much lower than the PETE. Sun has great exergy potential, and power

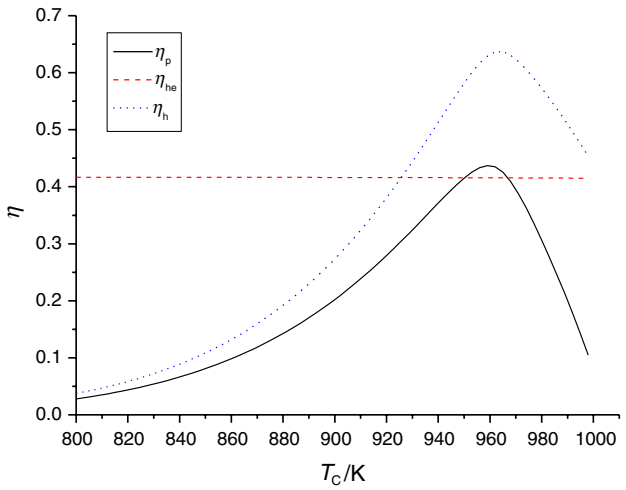

Fig. 3 Changes of energy efficiencies with cathode temperature

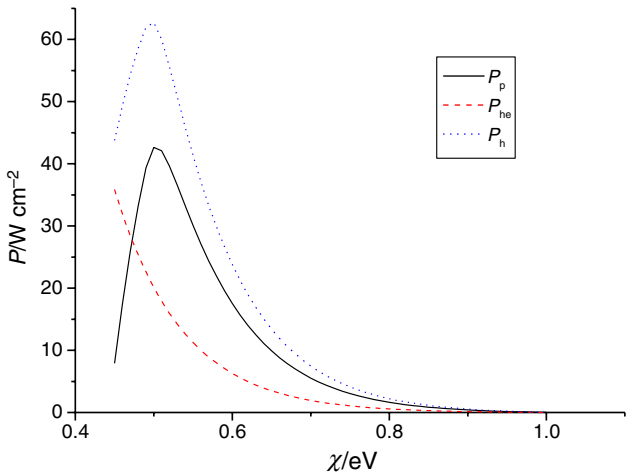

Fig. 5 Changes of power output densities with electron affinity

output from the considered system is so much lower, and it results in a great amount of exergy destruction.

In Figs. 5–7, variation in considered parameters with electron affinity is illustrated. The electron affinity of the cathode is another important variable since it is shown Eq. (16). The higher electron efficiency means the higher the work function of the cathode. For the electron conduction, electron energy needs to overcome work function, and, in this way, electrons can be conveyed to the anode. It is obvious that decreasing work function causes decreasing band gap and electron affinity. Power density changes are shown in Fig. 5. Like the effect of the cathode, temperature, density, and voltage values are inversely proportional and extremum points are possible. According to Fig. 5, power densities of the PETE and *H* reach a maximum point and then they begin to decrease. These points are obtained at 0.5 eV. This is the expected result because the higher electron affinity means higher cathode work function results in higher energy for electron emittance. When the power density of the HE is investigated, one can see that HE decreases with electron affinity. Since rejected heat from the PETE, which is transferred to HE as heat input of the system, reduces with electron affinity, this decreasing trend is very fast until the electron affinity is equal to 0.6 eV. Variation at the power density of HE is ranged from 35.781 to 0.008 W cm^{-2}. Energy efficiency rates are revealed in Fig. 6. Energy efficiencies of the PETE and *H* reach their maximum points at 0.5 eV, and the corresponding values are 0.426 and 0.627, respectively. The energy efficiency of the HE is constant at 0.416. Variations in exergy destruction rate densities are revealed in Fig. 7. Exergy destruction rate densities of the PETE and HE have minimum points. They are resulting from the same reasons explained in the previous paragraph. Corresponding values are 2.521 W cm^{-2} K^{-1} and 3.234 W cm^{-2} K^{-1}, respectively. The exergy destruction rate density of the HE reduces with

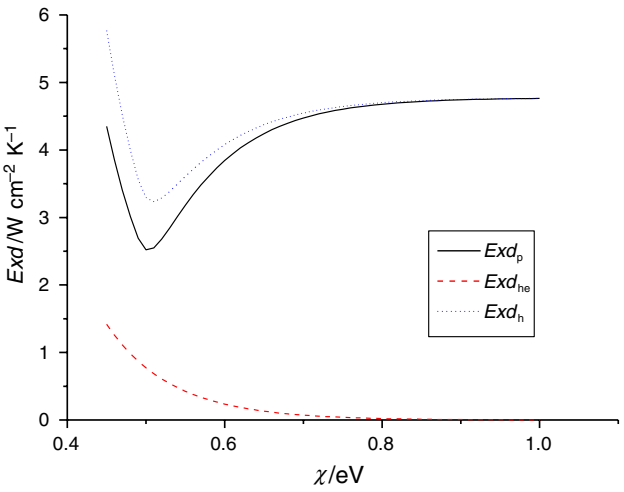

Fig. 7 Changes of exergy destruction raterate densities with electron affinity

the electron affinity. This reduction occurs from 1.420 to 0.00029 W cm^{-2} K^{-1}.

Variations in the parameters according to anode work function are depicted between Figs. 8–10. The work function of the anode affects the cathode temperature, so the greater anode work function causes the lower cathode temperature. The reason for this is that the electron population decreases with anode work function. These cases make anode work function another important variable for the PETE and HE. Power densities are depicted in Fig. 8. PETE and *H* have the extremum points, which are the maximum, such as others. The results show that they reach their maximum points at 0.64 eV for the PETE and 0.65 for the *H*. Corresponding values are 49.990 W cm^{-2} and 67.2948 W cm^{-2}, respectively. For the HE, power density grows up and it ranges from 1.687 to 39.092 W cm^{-2}. This change is linear after

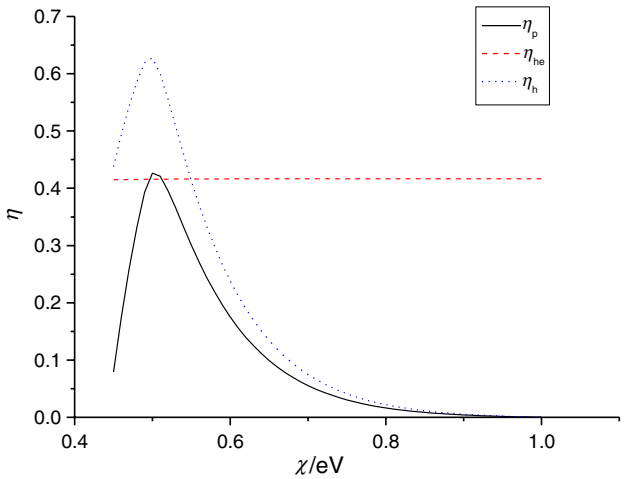

Fig. 6 Changes of energy efficiencies with electron affinity

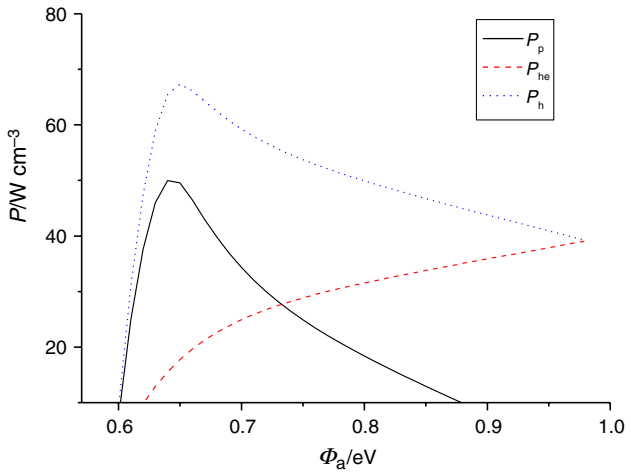

Fig. 8 Changes of power output densities with anode work function

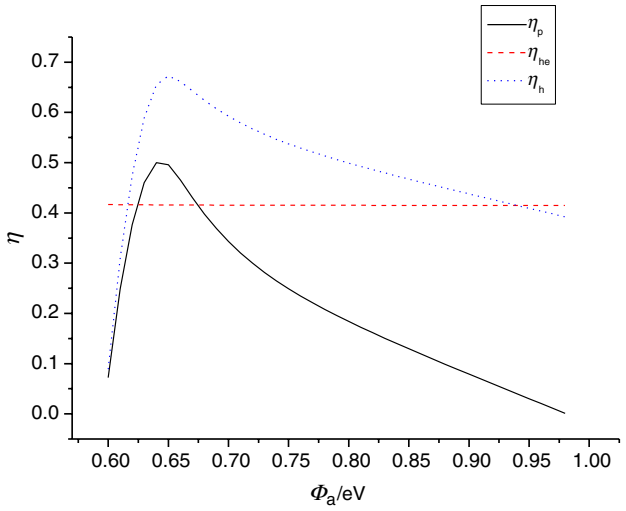

Fig. 9 Changes of energy efficiencies with anode work function

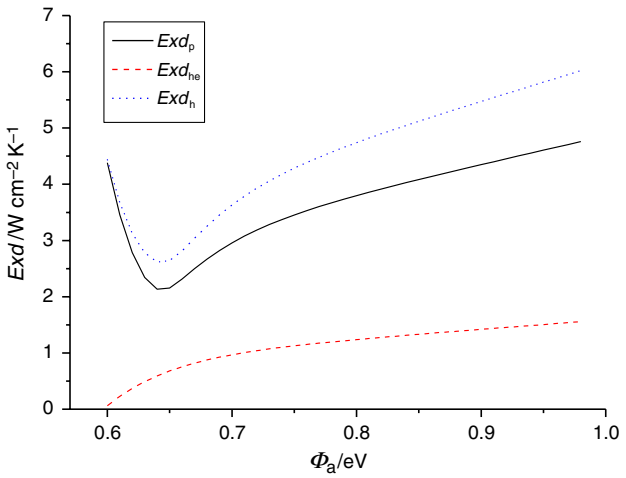

Fig. 10 Changes of exergy destruction raterate densities with anode work function

about 0.7 eV. Energy efficiencies of the PETE, HE, and H can be seen in Fig. 9. They have a similar tendency with power density change. Optimum points are 0.500 for the PETE and 0.673 for the H. Like other energy efficiencies, the energy efficiency of the HE can be assumed as constant at 0.416. When investigating exergy destruction, PETE and H have the minimum points which are equal to 2.134 W cm^{-2} K^{-1} and 2.617 W cm^{-2} K^{-1}, respectively. Finally, exergy destruction rate density of the HE ranges from 0.063 to 1.590 W cm^{-2} K^{-1}.

In Figs. 11–13, the variation in the exergetic parameters called ecological exergetic index, modified ecological exergetic index, exergy efficiency, depletion ratio, waste exergy ratio, and sustainability index is depicted according to cathode temperature, electron affinity, and anode work

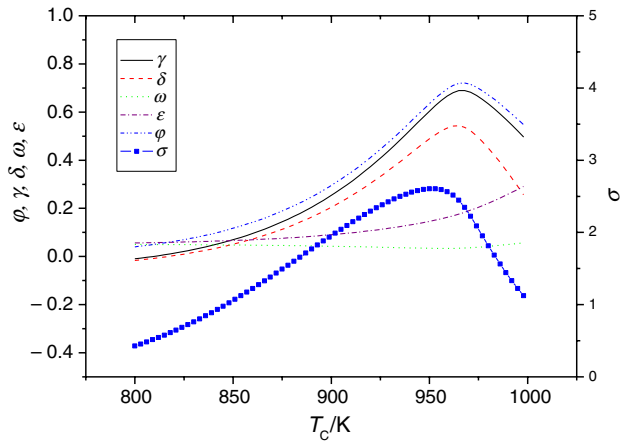

Fig. 11 Changes of exergetic indicators with anode cathode temperature

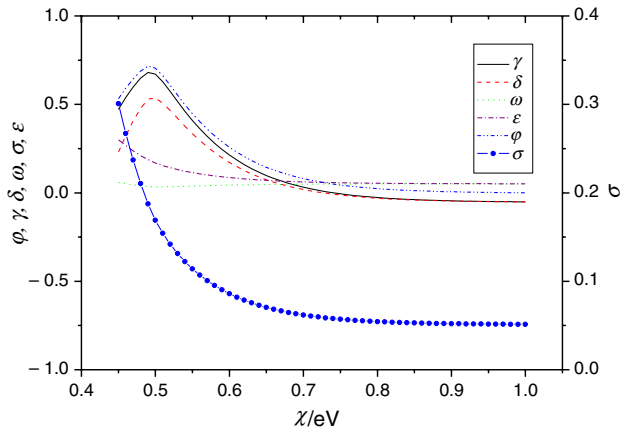

Fig. 12 Changes of exergetic indicators with electron affinity

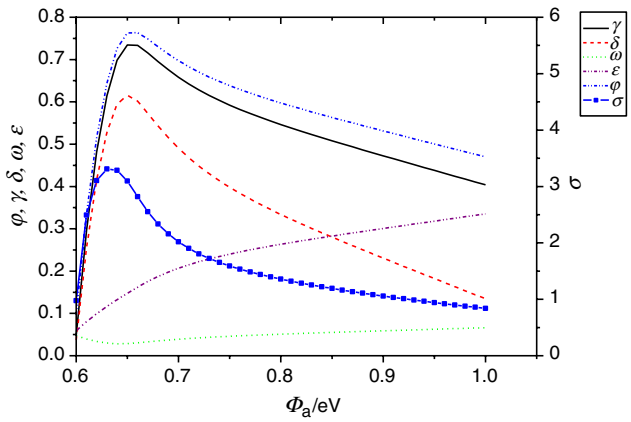

Fig. 13 Changes of exergetic indicators with anode work function

function for the hybrid system. Firstly, variations for the cathode temperature are investigated. Except for the depletion ratio and exergetic waste ratio, other parameters have maximum points. The depletion ratio has a minimum point when the waste exergy ratio grows up. This means that total exergetic losses of the exergy source are getting bigger with the cathode temperature for the waste exergy ratio, which is ranged from 0.0563 to 0.2917. Depletion ratio reaches its minimum at 959 K, and it is equal to 0.3341; this represents the portion of the destructed exergy of the fuel exergy. Exergetic ecological index and the modified exergetic ecological function reach their maximums at 974 K. Negative values represent where exergy destruction rate or total exergy losses are bigger than the power output and vice versa for positive values. Optimization of them can provide to determine the higher exergy efficiency and lower depletion ratio/exergetic losses. The maximum exergy efficiency is obtained at the 965 K. One can say that operation near the maximum power output point is advantageous about better performance and better exergetic values. At the maximum power and energy efficiency, the hybrid system can be used environmentally friendly and more sustainable. Secondly, the same variations are investigated for the electron affinity. Exergetic ecological index, modified exergetic ecological index, and exergy efficiency have maximum points. Exergetic ecological index and exergy efficiency have maximum points at the 0.49 eV, while the modified exergetic ecological index has the maximum point at the 0.5 eV. Depletion ratio has a minimum, and it reaches this value at 0.5 eV and sustainability index decreases continuously, which is ranged from 0.301 to 0.05128. Like the previous parameter, near the maximum power output system has good performance in terms of environmentally friendly and sustainability. Thirdly, research for the anode work function is performed. Exergetic ecological index, modified exergetic ecological index, exergy efficiency, and sustainability index have maximum points. Their maximums are obtained at 0.65 eV, 0.65 eV, 0.66 eV, and 0.63 eV, respectively. The depletion ratio has the minimum value at the 0.63 eV. These values are very close to the maximum power output and energy efficiency values. This means near the maximum performance values system operates sustainability and environmentally friendly.

In ref [31], PETE hybrid systems including Rankine, Stirling, and Brayton cycles as bottom cycles are considered. Their energy efficiencies are shown with changing cathode temperature. The results show that the maximum efficiency is obtained 60.3% for the PETE–Stirling hybrid system, 50.9% for the PETE–Rankine hybrid system and 40.2% for the PETE–Brayton hybrid system. Comparing these results to system considered in this study, 63.7% energy efficiency is possible to achieve and these results prove that PETE-based hybrid systems can be a strong alternative for electricity generation.

Conclusions

In this article, a PETE–HE hybrid system is investigated in terms of its performance and several exergetic indices. PETE–HE is chosen because PETE is efficient solar–electric converter. There is a possibility of the usage of the waste heat at a bottom cycle. Therefore, it was investigated whether an alternative cycle for electricity generation. According to the results, there are some points making its performance maximum and some points make the hybrid system provide to use it more sustainable and environmentally friendly. These points are very close, where the power output and energy efficiency are the maximum. It is recommended that for the high-performance and sustainable operation, some parameters are chosen as follows:

- 965 K for the cathode temperature
- 0.65 eV for the anode work function.

Corresponding values are obtained at optimum cathode temperature. Power output, energy efficiency, exergy efficiency, exergetic sustainability index, ecological, and modified ecological exergetic index are 63.698 W cm^{-2}, 0.637, 0.721, 2.603, 0.652, and 0.477, respectively. Similarly, corresponding values at the optimum anode work function are 67.295 W cm^{-2}, 0.673, 0.764, 3.312, 0.735, and 0.616, respectively.

For the future studies, economic, exergoeconomic, and techno-economic analyses should be done for the present feasibility of this kind of systems.

References

1. Schwede JW, Bargatin I, Riley DC, et al. Photon-enhanced thermionic emission for solar concentrator systems. Nat Mater. 2010;9:762–7.
2. Segev G, Rosenwaks Y, Kribus A. Efficiency of photon enhanced thermionic emission solar converters. Sol Energy Mater Sol Cells. 2012;107:125–30.
3. Reck K, Hansen O. Thermodynamics of photon-enhanced thermionic emission solar cells. Appl Phys Lett. 2014;104:023902.
4. Su S, Zhang H, Chen X, et al. Parametric optimum design of a photon-enhanced thermionic solar cell. Sol Energy Mater Sol Cells. 2013;117:219–24.
5. Su S, Wang Y, Liu T, et al. Space charge effects on the maximum efficiency and parametric design of a photon-enhanced thermionic solar cell. Sol Energy Mater Sol Cells. 2014;121:137–43.
6. Varpula A, Tappura K, Prunnila M. Si, GaAs, and InP as cathode materials for photon-enhanced thermionic emission solar cells. Sol Energy Mater Sol Cells. 2015;134:351–8.
7. Wang Y, Liao T, Zhang Y, et al. Effects of nanoscale vacuum gap on photon-enhanced thermionic emission devices. J Appl Phys. 2016;119:045106.
8. Segev G, Rosenwaks Y, Kribus A. Limit of efficiency for photon-enhanced thermionic emission vs. photovoltaic and thermal conversion. Sol Energy Mater Sol Cells. 2015;140:464–76.

9. Xiaoa G, Zheng G, Ni D, Li Q, Qiu M, Nia M. Thermodynamic assessment of solar photon enhanced thermionic conversion. Appl Energy. 2018;223:134–45.
10. Açıkkalp E, Yerel Kandemir S, Ahmadi MH. Performance evaluation of the thermophotovoltaic driven thermoionic refrigerator. J Energy Res Technol. 2020;142(3):032001.
11. Esen H, Inalli M, Esen M, Pihtili K. Energy, and exergy analysis of a ground-coupled heat pump system with two horizontal ground heat exchangers. Build Environ. 2007;42:3606–15.
12. Abdollahpour A, Ghasempour R, Kasaeian A, Ahmadi MH. Exergoeconomic analysis and optimization of a transcritical CO2 power cycle driven by solar energy based on nanofluid with liquefied natural gas as its heat sink. J Therm Anal Calorim. 2020;139:451–73.
13. Vakilabadi MA, Bidi M, Najafi AF, Ahmadi MH. Energy, exergy analysis and performance evaluation of a vacuum evaporator for solar thermal power plant zero liquid discharge systems. J Therm Anal Calorim. 2020;139:1275–90.
14. Ahmadi MH, Sadaghiani MS, Pourfayaz F, Ghazvini M, Mahian O, Mehrpooya M, Wongwises S. Energy and exergy analyses of a solid oxide fuel cell-gas turbine-organic rankine cycle power plant with liquefied natural gas as heat sink. Entropy. 2018;20(7):484.
15. Ashouri M, Mohammad HA, Pourkiaei SM, Astaraei FR, Ghasempour R, Ming T, Hemati JH. Exergy and exergo-economic analysis and optimization of a solar double pressure organic Rankine cycle. Therm Sci Eng Prog. 2018;6:72–86.
16. Mirzaei M, Ahmadi MH, Mobin M, Nazari MA, Alayi R. Energy, exergy and economics analysis of an ORC working with several fluids and utilizes smelting furnace gases as heat source. Therm Sci Eng Prog. 2018;5:230–7.
17. Naseri A, Bidi M, Ahmadi MH. Thermodynamic and exergy analysis of a hydrogen and permeate water production process by a solar-driven transcritical CO_2 power cycle with liquefied natural gas heat sink. Renew Energy. 2017;113:1215–28.
18. Naseri A, Bidi M, Ahmadi MH, Saidur R. Exergy analysis of a hydrogen and water production process by a solar-driven transcritical CO_2 power cycle with Stirling engine. J Clean Prod. 2017;158:165–81.
19. Noroozian A, Mohammadi A, Bidi M, Ahmadi MH. Energy, exergy and economic analyses of a novel system to recover waste heat and water in steam power plants. Energy Convers Manag. 2017;144:351–60.
20. Milad A, Ahmadi MH, Feidt M, Astaraei FR. Exergy and energy analysis of a regenerative organic Rankine cycle based on flat plate solar collectors. Mech Ind. 2017;18(2):217.
21. Vandani AMK, Joda F, Ahmadi F, Ahmadi MH. Exergoeconomic effect of adding a new feedwater heater to a steam power plant. Mech Ind. 2017;18(2):224.
22. Ahmadi MH, Mehrpooya M, Pourfayaz F. Thermodynamic and exergy analysis and optimization of a transcritical CO_2 power cycle driven by geothermal energy with liquefied natural gas as its heat sink. Appl Therm Eng. 2016;109:640–52.
23. Vandani AMK, Bidi M, Ahmadi MH. Energy, exergy and environmental analyses of a combined cycle power plant under part-load conditions. Mech Ind. 2016;17(6):610.
24. Ansarinasab H, Mehrpooya M, Sadeghzadeh M. An exergy-based investigation on hydrogen liquefaction plant-exergy, exergoeconomic, and exergoenvironmental analyses. J Clean Prod. 2019;210:530–41.
25. Mehrpooya M, Sadeghzadeh M, Rahimi A, Pourimanc M. Technical performance analysis of a combined cooling heating and power (CCHP) system based on solid oxide fuel cell (SOFC) technology—a building application. Energy Convers Manag. 2019;198:111767.
26. Ahmadi MH, Banihashem SA, Ghazvini M, Sadeghzadeh M. Thermo-economic and exergy assessment and optimization of performance of a hydrogen production system by using geothermal energy. Energy Environ. 2018;29(8):1373–92.
27. Angulo-Brown F. An ecological optimization criterion for finite-time heat engines. J Appl Phys. 1991;69:7465–9.
28. Yan Z. Comment on ecological optimization criterion for finite-time heat-engines. J Appl Phys. 1993;73:3583. E. Açıkkalp/ Energy Convers Manag. 2017; 132:432–437437.
29. Açıkkalp E, Ahmadi MH. Exergetic ecological index as a new exergetic indicator and an application for the heat engines. Therm Sci Eng Prog. 2018;8:204–10.
30. Açıkkalp E. Methods used for evaluation actual power generating thermal cycles and comparing them. Int J Electr Power Energy Syst. 2015;69:85–9.
31. Xiao G, Zheng G, Li MQQ, Li D. Nia M Thermionic energy conversion for concentrating solar power. Appl Energy. 2017;208:1318–42.